

Microdosimetric specific energy probability distribution in nanometric targets and its correlation with the efficiency of thermoluminescent detectors exposed to charged particles

Alessio Parisi^{a,b,*}, Olivier Van Hoey^a, Patrice Mégret^b, Filip Vanhavere^a

^a Belgian Nuclear Research Centre SCK·CEN, Mol, Belgium

^b University of Mons, Faculty of Engineering, Mons, Belgium



ARTICLE INFO

Keywords:

Microdosimetry
Thermoluminescence
Efficiency modelling
Specific energy
LiF:Mg,Ti
LiF:Mg,Cu,P
PHITS

ABSTRACT

Due to their common use for dose measurements in space and hadron therapy facilities, it is of fundamental importance to know the efficiency of luminescent detectors for measuring a wide range of particles and energies. However, due to experimental limitations it is often not possible to irradiate the detectors with very high energies, less common isotopes or exotic particles. Furthermore, the efficiency determination at low energies is biased with associated large uncertainties in range, linear energy transfer and dose. This paper presents the recently developed Microdosimetric d(z) Model able to assess the relative efficiency of thermoluminescent detectors for measuring different radiation qualities by relating the simulated dose probability distribution of the specific energy in nanometric targets with an experimentally determined response function. The model was tested in case of LiF:Mg, Ti (MTS) and LiF:Mg,Cu,P (MCP) thermoluminescent detectors exposed to charged particles from ¹H to ¹³²Xe in the energy range 3–1000 MeV/u. A comparison with experimentally determined efficiency results showed a very good agreement in case of calculations performed in a simulated target size of 40 nm. This validated model can be used to assess detector efficiency to exotic particles, unavailable radiation qualities and energies at ground level accelerators or complex mixed fields. The assumptions behind the model, its methodology and results are discussed in detail. Furthermore, a systematic investigation on the effect of simulation parameters on the calculated efficiency values is included in the manuscript.

1. Introduction

Because of their safe, light, small and passive nature (Olko, 2010), radiation detectors based on the thermoluminescence technique (McKeever, 1988; Chen and Pagonis, 2011; Bos, 2017) are commonly used for space dose mapping experiments (Reitz et al., 2005; Hajek et al., 2006; Szántó et al., 2015; Berger et al., 2016), astronaut personal dosimetry (Deme et al., 1999; Straube et al., 2010; Apáthy et al., 2002) stratospheric studies (Katona et al., 2007; Zábóri et al., 2016), in-phantom organ dose measurements inside and outside shuttles, the International Space Station and commercial flights (Yasuda, 2009; Berger et al., 2008, 2013), space dosimetry of biological experiments (Vanhavere et al., 2008; Berger et al., 2012, 2015), aircrew monitoring (Hajek et al., 2002; Bilski et al., 2004 a; Hajek et al., 2004), radiotherapy mailed audits (Kron, 1999; Kunst et al., 2017), in field (Geiß et al., 1998 b; Berger et al., 2006a) and out of field (Mukherjee et al., 2011; Knežević et al., 2017; Stolarczyk et al., 2018) dose assessment in

hadron therapy. However, radiation measurements in these complex radiation environments (Mayles et al., 2007; Bagshaw, 2008; Nelson, 2016) require an in depth knowledge of detector response in measuring a wide range of particles and energies.

Among all materials available, thermoluminescent detectors based on lithium fluoride are the most diffused and studied worldwide, especially in the form of lithium fluoride doped with magnesium and titanium (LiF:Mg,Ti) or with magnesium, copper and phosphorus (LiF:Mg,Cu,P) (Horowitz, 1993; McKeever et al., 1995; Bilski, 2002). The experimental investigation of the efficiency of these detectors has been carried out during the years by means of calibrated ion beam exposures at ground level particle accelerators (Horowitz, 1981; Benton et al., 2000; Berger et al., 2006b; Bilski, 2006; Berger and Hajek, 2008; Bilski and Puchalska, 2010; Bilski et al., 2011; Gieszczyk et al., 2013; Şadıl et al., 2015b; Parisi et al., 2017 b; Parisi et al., 2018).

Due to the complexity of the physical processes taking part in the thermoluminescent phenomenon (McKeever, 1988; Chen and Pagonis,

* Corresponding author. Belgian Nuclear Research Centre SCK·CEN, Mol, Belgium.

E-mail address: alessio.parisi@sckcen.be (A. Parisi).

<https://doi.org/10.1016/j.radmeas.2018.12.010>

Received 25 April 2018; Received in revised form 12 November 2018; Accepted 19 December 2018

Available online 21 December 2018

1350-4487/ © 2018 Elsevier Ltd. All rights reserved.

2011; Bos, 2017), the determination of an absolute luminescence efficiency η (Equation (1)), namely the ratio between the average energy emitted by the detector as form of light (ε_{TL}) and the mean energy imparted to the detector by the radiation field (ε), is biased by intrinsic difficulties.

$$\eta = \frac{\varepsilon_{TL}}{\varepsilon} \quad (1)$$

Consequently, during the years researchers focused their efforts in the determination of the relative luminescence efficiency η_{rel} . The latter quantity is defined as in Equation (2) as the intensity of the luminescence signal S per unit of absorbed dose D for the radiation under investigation over the same quantity for a reference radiation.

$$\eta_{rel} = \frac{\left(\frac{S}{D}\right)_{radiation}}{\left(\frac{S}{D}\right)_{reference\ radiation}} \quad (2)$$

It was concluded that this relative efficiency is not a unique function of the linear energy transfer (LET) of the incident radiation, but depends strongly also on the particle type (Horowitz, 1981; Berger et al., 2006b; Berger and Hajek, 2008). This happens because, in order to have the same LET, two different particles must have different velocities: the heavier the particle, the higher the velocity. Consequently, the heavier particle will produce δ -rays with higher energies (so longer range in matter) which will deposit their energy in a radially less dense way around the track of the charged particle (Olko, 2007). It follows that, being the response of the detector generally inversely related to the energy deposition density of the impinging radiation, the efficiency of the detector in measuring two different particles characterized by the same LET value will be higher for the heavier particle.

Unfortunately, the experimental determination of the relative efficiency of luminescent detectors through irradiations in charged particle accelerators is time consuming and very expensive. Furthermore, due to technical limitations it is often not possible to irradiate the detectors with energies above 1 GeV/u or with less common isotopes. In addition, the efficiency determination for low energies is biased with big uncertainties of all parameters (i.e. LET, range, absorbed dose). However, a complete characterization of the efficiency of these detectors is needed, especially for space applications where particles with a really broad energy spectrum and exotic isotopes are present. As consequence, during the years, many models have been developed in order to explain and predict the efficiency of thermoluminescent detectors for different radiation qualities. Among all of them, the most common ones are based on track structure theory (Larsson and Katz, 1976; Waligórski and Katz, 1980; Kalef-Ezra and Horowitz, 1982; Geiß et al., 1998 a; Ávila et al., 1999; Boscolo et al., 2015). Two ingredients are needed for those calculations: the radial dose distribution and a dose response function. The first one can be evaluated through analytical models (Butts and Katz, 1967; Faïn et al., 1974; Waligórski et al., 1986; Katz et al., 1990; Katz et al., 1996; Chen and Kellerer, 1997; Cucinotta et al., 1997; Geiß et al., 1998 a, Greilich et al., 2014) or Monte Carlo simulations (Krämer and Kraft, 1994; Waligórski et al., 1986; Ávila et al., 1996) and represents the dose distribution around the track of the particle while traveling through the detector. The second one represents the response of the detector when irradiated at different dose levels with a sparsely ionizing radiation such as photons or electrons (Horowitz, 1990; Gamboa-deBuen et al., 1998, Bilski, 2002, Massillon-Jl et al., 2006, Bilski et al., 2007, Massillon-Jl et al., 2011).

In depth studies were performed to investigate how the assessment of the radial dose distribution and the dose response function could affect the calculated efficiency (Ávila and Brandan, 2002; Ávila et al., 2008, Massillon-Jl et al., 2011). Efficiency values were determined for response functions obtained exposing the detectors to 8.1 keV X-rays, β -particles, 100 keV X-rays and photons from a ^{60}Co γ -ray source. Furthermore, artificial response functions were also included in the study. On the other hand, the radial dose distribution was evaluated by means

of both analytical formulations or Monte Carlo simulations. It was concluded that, for all radial dose distribution and dose response function combinations, the quantitative agreement between the calculated and the experimental efficiency values was poor (Massillon-Jl et al., 2011). Similar conclusions were drawn in a separate work (Horowitz et al., 2012) which underlined the necessity of improving the evaluation of the radial dose distribution, i.e. implementing accurate models for the transport of low energy ions and secondary electrons, and reducing the uncertainties associated with the assessment of the dose response function at high dose levels. Furthermore, as the concept of radial dose distribution is inapplicable to photons, neutrons or electrons, one should remember that track structure models cannot be applied for efficiency determination for these radiation qualities (Olko et al., 2002b).

However, an alternative approach based on microdosimetry (International Commission on Radiation Units and Measurements, 1983; Kellerer, 1985; Rossi and Zaider, 1996) was proposed by Olko (Olko, 2002a; Olko, 2002b; Olko, 2004; Olko, 2007). The key idea of his methodology was to use microdosimetric specific energy probability distributions in place of radial dose distributions to quantify the changes in the local ionization density. The detector is supposed being composed by many independent structures, called targets, which act as sensitive volumes for measuring radiation. The size of these targets is a free parameter in Olko's methodology.

In Olko's model, the relative efficiency was evaluated using Equation (3) as the ratio of the specific energy frequency probability distribution $f(z)$ folded into a specific energy response function $r(z)$, over the same quantity for a reference radiation. The factor $1/\bar{z}_F$ was used to change the normalization from per single event to per unit of dose (Olko, 2002a). Here and in the following, probability distributions and expectation values are relative to single event microdosimetric spectra (International Commission on Radiation Units and Measurements, 1983).

$$\eta_{rel} = \frac{\left[\frac{1}{\bar{z}_F} \int_0^{+\infty} f(z) r(z) dz \right]_{radiation}}{\left[\frac{1}{\bar{z}_F} \int_0^{+\infty} f(z) r(z) dz \right]_{reference\ radiation}} \quad (3)$$

The reference radiation was chosen to be the photons from a ^{137}Cs γ -ray source and \bar{z}_F is the frequency mean specific energy defined as in Equation (4) (International Commission on Radiation Units and Measurements, 1983).

$$\bar{z}_F = \frac{\int_0^{+\infty} z f(z) dz}{\int_0^{+\infty} f(z) dz} \quad (4)$$

The frequency distribution of the specific energy $f(z)$ induced by charged particles was assessed using an analytical approach (Olko and Booz, 1990) obtained parametrizing the results of simulations performed with the MOCA-14 code (Paretzke, 1988). In case of photons, the initial distribution of secondary electrons was calculated using the Monte Carlo code PHOEL-2 (Turner et al., 1980). Afterwards, electron track structure simulations were performed using the TRION code (Lappa et al., 1993) for obtaining the microdosimetric probability distributions. All the calculations were performed in an infinitesimal layer of water (the slowing down of the particle within the real detector was neglected) and the results were afterwards converted from targets in water to lithium fluoride using a density scaling approach. More details can be found elsewhere (Olko, 1989; Olko, 2002a; Olko, 2002b). Olko's model was used to calculate the efficiency of several detector types for measuring photons (Olko and Waligórski, 2002; Olko et al., 2002a; Olko et al., 2006) and charged particles from ^1H to ^{16}O with a maximum energy of 20 MeV/u (Olko et al., 2002b; Olko et al., 2004; Olko et al., 2006).

A similar model, called Microdosimetric $d(z)$ Model, has been recently developed using the Monte Carlo Particle and Heavy Ion

Transport code System (PHITS, Sato et al., 2018) in order to extend the validity of the microdosimetric approach to energies and particles relevant for hadron therapy and space applications. Differences with Olko's model can be found in the formalism used in evaluating the relative efficiency, the assessment of the microdosimetric probability distributions, the specific energy response function and the reference radiation. Furthermore, in this work, the particle slowing down within the detector and the creation of secondary particle were considered in the Monte Carlo calculations. The model was shortly presented in Parisi et al. (2017) c, Parisi et al. (2017) d together with a preliminary comparison between its results for target sizes of 10, 40 and 100 nm and experimental data from the Institute of Nuclear Physics (IFJ, Krakow, Poland: Bilski, 2006, Bilski and Puchalska, 2010, Bilski et al., 2011, Gieszczyk et al., 2013 and Sądziel et al., 2015b) for LiF:Mg, Ti (MTS) and LiF:Mg,Cu,P (MCP) detectors. In this paper, the Microdosimetric $d(z)$ Model is presented in detail including a complete description of the methodology used for the assessment of the dose distribution of the specific energy, an in depth comparison between results of the model in case of 10, 20, 30, 40 and 50 nm target sizes and experimentally determined efficiency data including results also from the Belgian Nuclear Research Centre (SCK•CEN, Mol, Belgium: Parisi et al., 2017 a and Parisi et al., 2018), the German Aerospace Centre (DLR, Cologne, Germany: Berger and Hajek, 2008) and the Atomic Institute (ATI, Vienna, Austria: Berger et al., 2006b and Berger and Hajek, 2008), a comparison between the methodology used for assessing LET values using the Monte Carlo code PHITS (Sato et al., 2018) with a similar approach employing the Stopping and Range of Ions in Matter (SRIM) software suite (Ziegler et al., 2010) and a systematic analysis on the effect of simulation parameters on the final calculated relative efficiency values.

2. Methodology

The relative luminescence efficiency of the detectors was evaluated using Equation (5), where $d(z)$ is the dose probability distribution of the specific energy and $r(z)$ is the specific energy response function.

$$\eta_{rel} = \frac{[\int_0^{+\infty} d(z) r(z) dz]_{radiation}}{[\int_0^{+\infty} d(z) r(z) dz]_{reference\ radiation}} \quad (5)$$

Differently from Olko's methodology (Olko, 2002a), the reference radiation was chosen to be the photons from a ^{60}Co γ -ray source instead of a ^{137}Cs γ -ray source. This was done because:

a. The most recent and complete set of high dose data present in literature for LiF:Mg, Ti (MTS) and LiF:Mg,Cu,P (MCP) thermoluminescent detectors and protocols of interest was available in case of a ^{60}Co γ -ray source (Bilski et al., 2007). Furthermore, that paper includes results also for high-LET optimized LiF:Mg, Ti thermoluminescent detectors with modified dopant concentration (MTT, Bilski et al., 2004 b) which in future can be used for modelling the efficiency of the latter detector type.

b. ^{60}Co γ -rays is the radiation quality currently being used at the Belgian Nuclear Research Centre SCK•CEN for calibration purposes and as reference radiation for relative efficiency determination (Berger et al., 2016; Parisi et al., 2017 a; Parisi et al., 2017 b; Parisi et al., 2018).

All the results present in this work refer to relative luminescence efficiency values corrected for medium choice (i.e. dose values calculated taking into account the material composing the detector), particle energy loss while traversing the detector, irradiated volume and self-absorption of the emitted light. Eventual experimental corrections needed for an adequate comparison of the experimental data with the results of the model should be performed by the experimental investigators (Bilski and Budzanowski, 2001; Sądziel et al., 2015a; Parisi et al., 2018).

2.1. Specific energy dose probability distribution – $d(z)$

The dose probability distribution of the specific energy $d(z)$ has been assessed performing computer radiation transport simulations with the Monte Carlo Particle and Heavy Ion Transport code System (PHITS) version 2.82 (Niita et al., 2006; Sato et al., 2013, 2015, 2018). The methodology is summarized hereunder.

a. The detector (^7Li fluoride cylinder, density = 2.5 g/cm³, diameter = 4.5 mm, thickness = 0.9 mm) was irradiated with charged particle mono-energetic beams (diameter = 9 mm, energy = 3, 5, 7, 10, 15, 20, 30, 40, 50, 60, 70, 80, 90, 100, 125, 150, 250, 500 and 1000 MeV/u) of ^1H , ^4He , ^{12}C , ^{16}O , ^{20}Ne , ^{28}Si , ^{40}Ar , ^{56}Fe , ^{84}Kr and ^{132}Xe ions or with a dual-energy (1173.2 and 1332.5 keV) photon beam representing the reference ^{60}Co γ -ray source. In all cases, the beam was impinging perpendicularly the base of the cylinder. Following the charged particle therapy PHITS input file recommendations (<https://phits.jaea.go.jp/lec/recommendation.zip>), which closely represent the situation of this work (precise assessment of dose, LET and microdosimetric distributions from charged particles), the energy straggling was considered using the Landau Vavilov formula (Vavilov, 1957) and the angular straggling was taken into account through the use of the Lynch's Coulomb diffusion formula (Lynch and Dahl, 1991) based on Moliere theory (Moliere, 1948). The Electron Gamma Shower version 5 (EGS5) code (Hirayama et al., 2005) was employed to simulate the transport of photons, electrons and positrons. The energy loss of charged particles, with the only exception of electrons and positrons, was assessed by means of the stopping power calculation model SPAR (Armstrong and Chandler, 1973) under the continuous slowing down approximation. The simulation cutoff for the transport of all ions was set to 1 MeV/u. A systematic analysis of the effect of simulation parameters on the calculated relative efficiency values is presented in Section 3.2 of this manuscript. For each particle-energy combination, a total number of 2×10^7 histories was simulated.

b. In order to take into account the particle slowing down, the assessment of the microdosimetric probability distributions was performed at different depths within the detector. The latter was divided in cylindrical computational subdomains (diameter = 4.5 mm, thickness = 1 μm) where the calculations were carried out. In each subdomain, the dose probability distribution of the specific energy was evaluated by means of the microdosimetric function (Sato et al., 2006, 2012) implemented in the Monte Carlo code PHITS. As done for Olko's analytical approach (Olko and Booz, 1990), Monte Carlo track structure simulations were performed and the results were used to develop an analytical function valid for a wide variety of particle, energy and site size combinations. The energy deposition in the core region of the particle track (Chatterjee and Schaefer, 1976) was assumed to be uniform and was determined using the stopping power code ATIMA (<http://web-docs.gsi.de/~weick/atima>). On the other hand, the production of δ -rays was considered accordingly to Butts, and Katz (1967) and the obtained spectrum was used as input for Monte Carlo calculations using the track structure code TRACEL (Tomita et al., 1997). The so developed analytical function has been applied for the analysis of cell survival fractions after radiation exposures (Sato et al., 2010; Sato and Furusawa, 2012; Sato and Hamada, 2014) and to simulate the microdosimetric probability distributions measured with tissue equivalent proportional counters (Tsuda et al., 2012, 2016). To the best of the authors' knowledge, this work represents the first time that this analytical approach is being used in the field of solid state physics. Knowing the energy spectra of the incident and secondary particles as function of detector depth, the microdosimetric probability distributions were evaluated in each subdomain in which the macroscopic detector was subdivided. The process was carried out for a large number of site sizes ranging from 1 nm to 2 μm . It is worth remembering that, in order to use this analytical approach for the calculation of microdosimetric probability distributions, the generation of ion's δ -rays should not be considered otherwise their contribution is

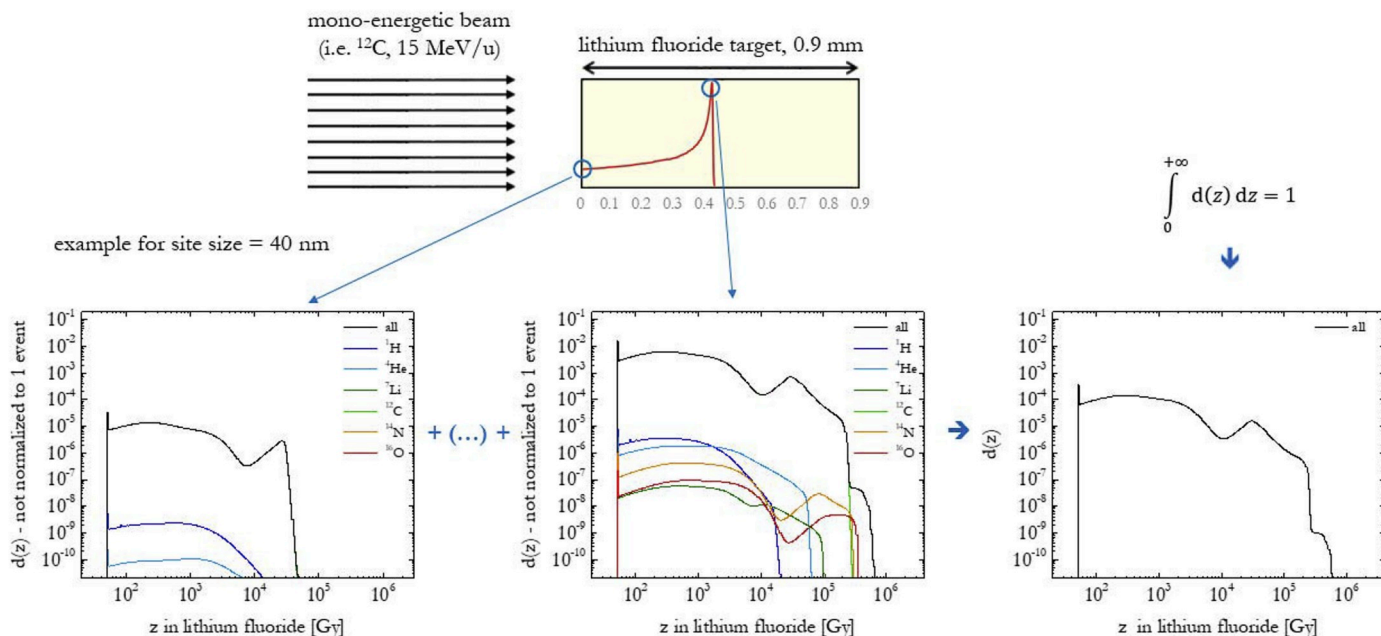


Fig. 1. Schematic representation of the methodology used to assess the average specific energy dose probability distribution over the detector volume in case of 15 MeV/u ^{12}C ions and a site size of 40 nm.

double counted (PHITS manual, <https://phits.jaea.go.jp/ririki-manuale.html>).

c. The obtained microdosimetric spectra were then summed and the resulting probability distribution was normalized to one event. A schematic representation of this process can be found in Fig. 1 in case of 15 MeV/u ^{12}C ions and a site size of 40 nm. The microdosimetric dose probability distributions are plotted as function of the specific energy for two subdomains: the first one at the entrance of the particle in the detector and the second one close to the particle stop. Although the microdosimetric probability distributions of only selected secondary fragments (^1H , ^4He , ^7Li , ^{14}N and ^{16}O ions) are plotted in Fig. 1 for the sake of clarity, the contribution of all secondary particles was included in the calculations. A logarithmic scale for $d(z)$ was chosen to enhance the visibility of fragment contribution. The final microdosimetric spectrum averaged on detector volume after normalization to one event is also plotted in Fig. 1.

As an example, Fig. 2 compares the dose probability distributions, averaged over the detector volume, induced by the lowest (^1H ions, 1000 MeV/u) and the highest (^{132}Xe ions, 3 MeV/u) LET particles included in this work. The spectra are presented in the form of $zd(z)$ (linear scale) vs z (logarithmic scale) which is the standard representation of a microdosimetric spectrum (Rossi and Zaider, 1996) where the area between two specific energy values is proportional to the fraction of macroscopic absorbed dose delivered in that specific energy range. This representation was not used in Fig. 1 in order to allow an easier visualization of fragment contribution. In both Figs. 1 and 2, the peak around 50 Gy represents the specific energy relative to one event of one ionization in site size of 40 nm.

2.2. Specific energy response function – $r(z)$

The microdosimetric model of this work shares with Olko's model (Olko, 2002a) the assumption that the macroscopic dose response function $R(D)$ can be applied as microdosimetric specific energy response function $r(z)$. For microscopic volumes and a large number of events, it can be assumed that the energy is distributed almost uniformly in the site. This is especially valid for sparsely ionizing radiations such high energy photons. As the macroscopic dose response function $R(D)$ is generally being experimentally evaluated with

relatively high dose values from a sparsely ionizing radiation, it follows that a large number of events occurs in the microscopic site. Consequently, the average value of the multi-event dose-dependent probability distribution of the specific energy z (International Commission on Radiation Units and Measurements, 1983; Kellerer, 1985; Rossi and Zaider, 1996), that for high dose values is a Gaussian shape distribution centered on the absorbed dose value D (Rossi et al., 1961), can be assumed being close to the one of the macroscopic absorbed dose D . Under this assumption, the macroscopic dose response function $R(D)$ can be used in first approximation as the microdosimetric specific energy response function $r(z)$.

Thus, in this work the linearity index of LiF:Mg, Ti (MTS) and LiF:Mg,P detectors exposed to ^{60}Co γ -rays was chosen as response function. This parameter is defined as in Equation (6) as the ratio between the luminescence intensity S per unit of dose D over the same

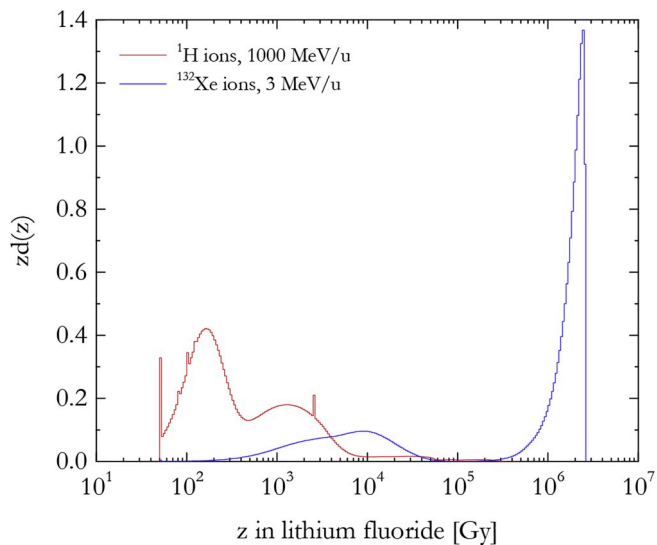


Fig. 2. Microdosimetric $zd(z)$ vs z spectra induced in a 40 nm site size by the lowest (1000 MeV/u ^1H) and the highest LET (3 MeV/u ^{132}Xe) particles included in this work.

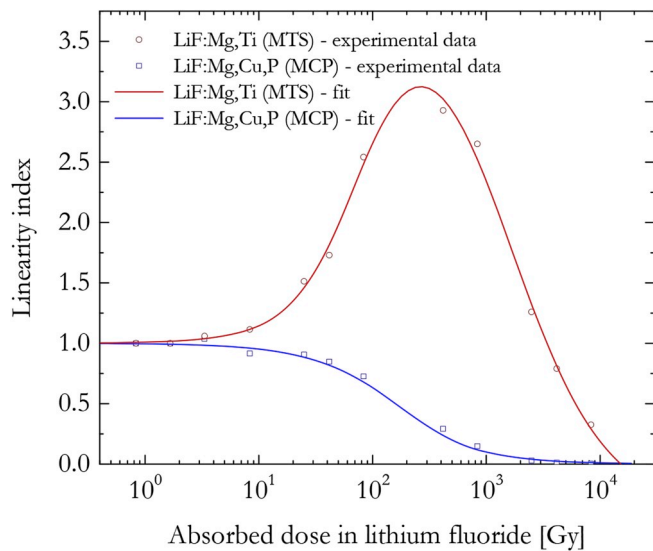


Fig. 3. Experimental macroscopic dose response function for the main peak of LiF:Mg, Ti (MTS) and LiF:Mg,Cu,P (MCP) thermoluminescent detectors exposed to ^{60}Co γ -rays (Bilski et al., 2007) and the fits used in the model.

quantity for a reference dose lying in the linear response of the detector. In the dose range over which the detector has a linear behavior, this parameter is equal to 1. On the other hand, the linearity index is smaller or greater than 1 in case of respectively sublinear or supralinear response.

$$\text{Linearity index} = \frac{\left(\frac{S}{D}\right)_{\text{dose}}}{\left(\frac{S}{D}\right)_{\text{reference dose}}} \quad (6)$$

The experimental data were extracted from Bilski et al. (2007) and converted from dose in water to dose in lithium fluoride by using a conversion coefficient of 0.833 obtained from the ratio between the mass energy absorption coefficients for lithium fluoride and water in case ^{60}Co γ -ray exposure. The latter values were extracted from the mass attenuation and mass energy absorption tables (Hubbell and Seltzer, 2004) of the National Institute of Standards and Technology (NIST, Maryland, United States of America). In Fig. 3, the linearity index of LiF:Mg, Ti (MTS) and LiF:Mg,Cu,P (MCP) detectors is plotted as function of the dose in lithium fluoride together with the fits used in the model.

2.3. Linear energy transfer – LET

For each particle-energy combination, the primary beam unrestricted frequency mean LET (International Commission on Radiation Units and Measurements, 1970) in lithium fluoride averaged on the particle track within the detector was assessed using the Monte Carlo code PHITS. This was done to allow an easier comparison of model's results with literature experimentally determined efficiency data, usually presented as function of this quantity. The procedure of averaging over the detector volume is similar to the one of Section 2.2 for the specific energy, but using the stopping power calculation model SPAR (Armstrong and Chandler, 1973) in place of the microdosimetric analytical function (Sato et al., 2006) and excluding fragment contributions.

This methodology was validated comparing the obtained LET values with the ones calculated with the Monte Carlo code Transport of Ions in Matter (TRIM) included in the Stopping and Range of Ions in Matter (SRIM) software suite version 2013.00 (Ziegler et al., 2010). In the latter case, the mono-energetic particle beam was impinging

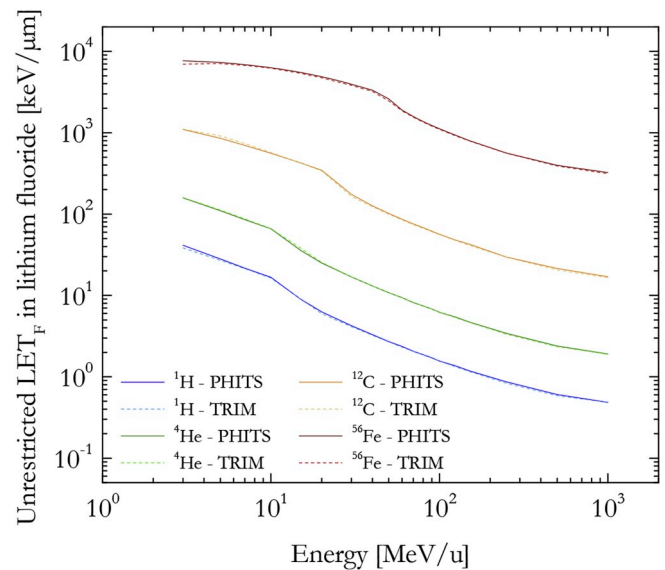


Fig. 4. Comparison between the primary beam unrestricted LET in lithium fluoride averaged on the particle track within the detector evaluated with PHITS and SRIM in case of ^1H , ^4He , ^{12}C and ^{56}Fe ions in the energy range 3–1000 MeV/u. The average value of the relative deviation between the results of the two codes was 2%.

perpendicularly a 0.9 mm thick layer of lithium fluoride. The fluence mean unrestricted LET_F was evaluated as function of depth and after that averaged on the particle track within the target. Fig. 4 compares the primary beam unrestricted LET in lithium fluoride averaged on the particle track within the detector evaluated with PHITS and SRIM in case of ^1H , ^4He , ^{12}C and ^{56}Fe ions in the energy range 3–1000 MeV/u. As it can be seen, a very good agreement was found between the codes, confirming the solidity of the calculations. The average relative deviation between the LET values determined using PHITS and TRIM, defined as in Equation (7), was found to be 2%. The maximum relative deviation was observed in case of 3 MeV/u ^{56}Fe ions, being 9%.

$$\text{Relative deviation} = \frac{|\text{LET}_{\text{PHITS}} - \text{LET}_{\text{TRIM}}|}{\text{LET}_{\text{PHITS}}} \quad (7)$$

Finally, a fixed conversion coefficient of 2.1 was used to convert LET values in lithium fluoride to LET in water. The latter value represents the average ratio between the unrestricted LET in lithium fluoride and water as function of the particle type and its energy (Parisi et al., 2018). If not differently specified, all LET values refer to fluence mean unrestricted LET in water.

3. Results

3.1. Relative luminescence efficiency of LiF:Mg, Ti (MTS) and LiF:Mg,Cu,P (MCP) detectors

Using Equation (5), the relative efficiency of LiF:Mg, Ti (MTS) and LiF:Mg,Cu,P (MCP) detectors for measuring particles from ^1H to ^{132}Xe was determined in the energy range 3–1000 MeV/u as function of the microdosimetric site size. The site sizes in which the Monte Carlo simulations were performed ranged from 1 nm to 2 μm . The obtained efficiency values were compared with experimental data from literature (Berger et al., 2006b; Bilski, 2006; Berger and Hajek, 2008; Bilski and Puchalska, 2010; Bilski et al., 2011; Gieszczyk et al., 2013; Saqdel et al., 2015b; Parisi et al., 2017 b; Parisi et al., 2017 a; Parisi et al., 2018) in order to investigate the existence of a possible optimal site size which can be used to predict the response of the detectors for measuring different radiation qualities.

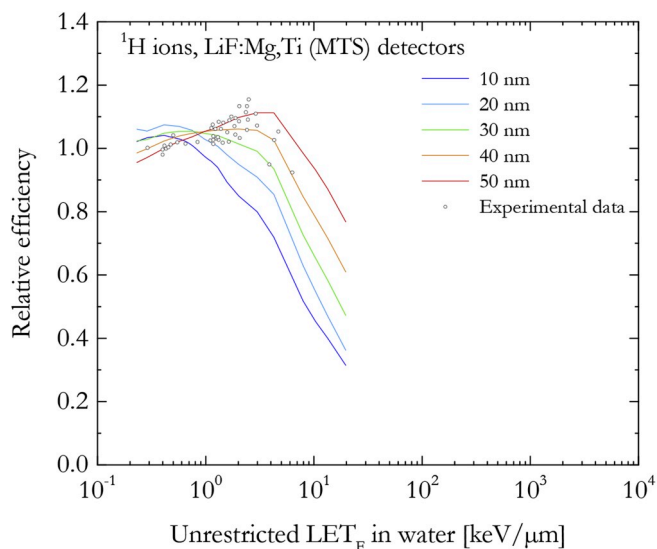


Fig. 5. Effect of changing the site size on the calculated relative efficiency values of LiF:Mg, Ti (MTS) detectors exposed to ^1H ions. Experimental efficiency data from [Şadel et al. \(2015b\)](#) and [Parisi et al. \(2018\)](#).

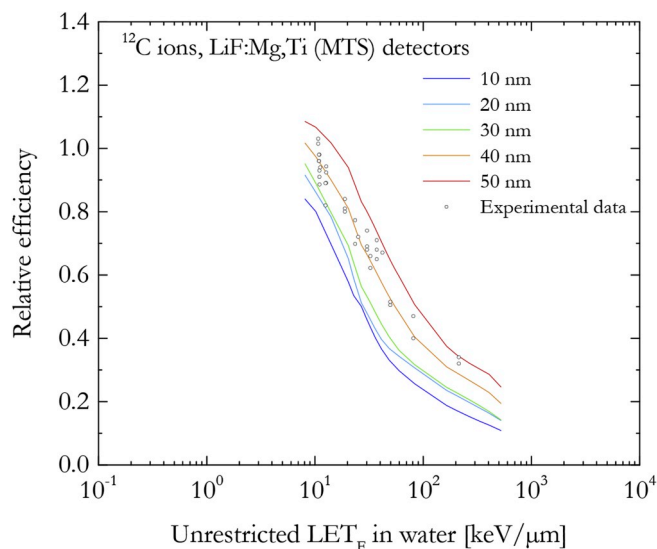


Fig. 7. Effect of changing the site size on the calculated relative efficiency values of LiF:Mg, Ti (MTS) detectors exposed to ^{12}C ions. Experimental efficiency data from [Berger et al. \(2006b\)](#), [Bilski \(2006\)](#), [Berger and Hajek \(2008\)](#), [Bilski and Puchalska \(2010\)](#), [Bilski et al. \(2011\)](#) and [Parisi et al. \(2017\)](#) a.

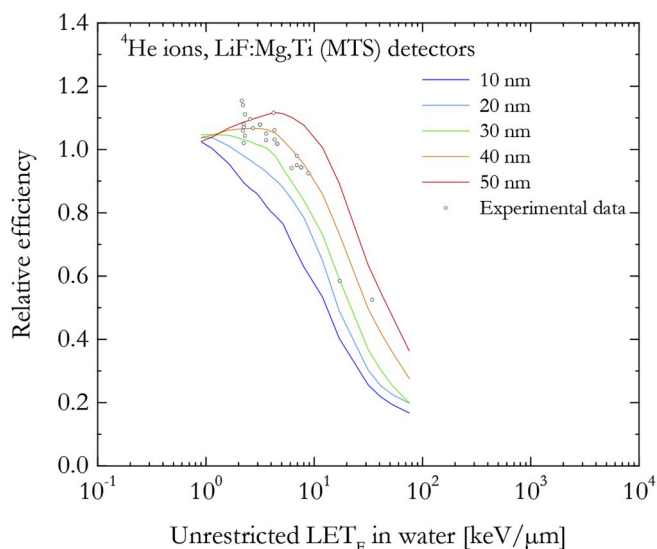


Fig. 6. Effect of changing the site size on the calculated relative efficiency values of LiF:Mg, Ti (MTS) detectors exposed to ^4He ions. Experimental efficiency data from [Berger et al. \(2006b\)](#), [Bilski \(2006\)](#), [Berger and Hajek \(2008\)](#), [Bilski and Puchalska \(2010\)](#), [Bilski et al. \(2011\)](#), [Parisi et al. \(2017\)](#) a and [Parisi et al. \(2018\)](#).

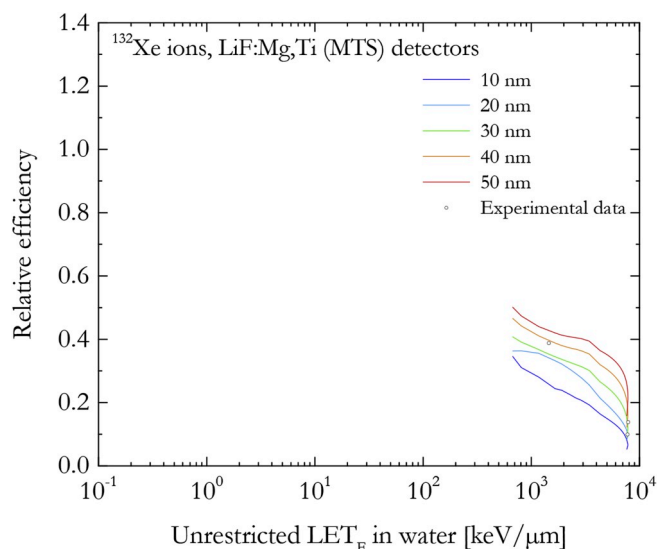


Fig. 8. Effect of changing the site size on the calculated relative efficiency values of LiF:Mg, Ti (MTS) detectors exposed to ^{132}Xe ions. Experimental efficiency data from [Bilski and Puchalska \(2010\)](#) and [Gieszczyk et al. \(2013\)](#).

As an example, [Figs. 5–8](#) show a comparison of the results of the model in case of LiF:Mg, Ti (MTS) detectors exposed to ^1H , ^4He , ^{12}C and ^{132}Xe for calculations performed in site sizes ranging from 10 to 50 nm. In these plots, the relative luminescence efficiency of the detectors is plotted as function of the fluence mean primary beam unrestricted LET in water. A similar comparison was performed for all particles and site sizes for both LiF:Mg, Ti (MTS) and LiF:Mg,Cu,P (MCP) detectors. Notwithstanding the large spread of experimental results especially in case of ^1H and ^4He ions, for both detector types and all ions the best agreement between the results of the Microdosimetric d(z) Model and experimental data was found in case of calculations performed in a site size of 40 nm. Thus, the results of the Microdosimetric d(z) Model for a site size of 40 nm are plotted in [Figs. 9 and 10](#) together with experimental efficiency values from literature for LiF:Mg, Ti (MTS) and LiF:Mg,Cu,P (MCP) detectors respectively. As it can be seen, a very

good agreement was found for all particles and energies included in this study. These results are summarized in [Figs. 11 and 12](#) in which the relative efficiency of the two detector types is plotted as function of the fluence mean primary beam unrestricted LET in water and the particle type. The model is able to accurately describe the not unique dependence of the relative luminescence efficiency occurring due to the phenomena described in [Section 1](#) of this manuscript.

The interpretation of the physical meaning of the dimension of the radiation sensitive size evaluated through the microdosimetric analysis has been topic of discussion for years ([Horowitz, 1999](#); [Olko, 2002a](#); [Olko, 2007](#)). The value of 40 nm assessed in this work for both LiF:Mg,Cu,P (MCP) and LiF:Mg, Ti (MTS) thermoluminescent appears to be much larger than the lithium fluoride lattice constant (~ 0.4 nm [Hutchison and Johnston, 1940](#)) and the average distance between Mg-based trapping structures ($\sim 1\text{--}3$ nm) in these LiF based crystals ([Horowitz, 1999](#)). Consequently, it is proposed to represent an average

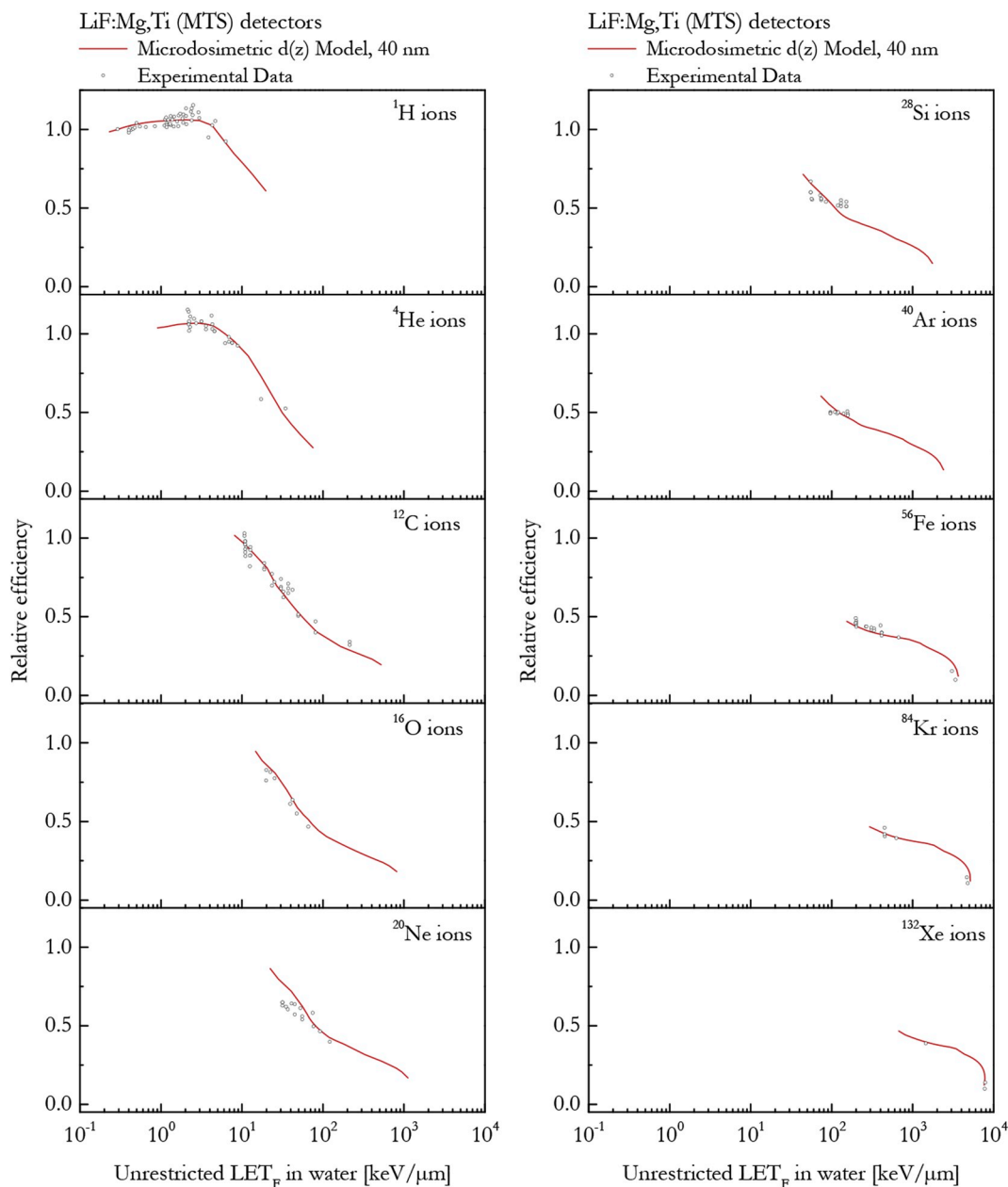


Fig. 9. Results of the Microdosimetric $d(z)$ Model in case of LiF:Mg, Ti (MTS) detectors for a site size of 40 nm in comparison with experimental data from Berger et al. (2006b), Bilski (2006), Berger and Hajek (2008), Bilski and Puchalska (2010), Bilski et al. (2011), Gieszczyk et al. (2013), Sądel et al. (2015b), Parisi et al. (2017) a and Parisi et al. (2018).

charge migration distance during the recombination stage which was previously determined to be 40–47.5 nm for LiF:Mg, Ti (MTS) detectors (Horowitz et al., 1996; Horowitz, 2001). Alternatively, recent X-ray diffraction investigations have proven the LiF:Mg, Ti (MTS) crystallite size being 31 nm (Roomi et al., 2018), value which is close to the target dimension assessed by the microdosimetric analysis of this study (40 nm) and the previous analysis by Olko (24 nm, Olko, 2002a).

3.2. Effect of simulation parameters on the calculated relative luminescence efficiency values

The effect of changing the simulation parameters on the calculated relative efficiency values, both in the definition of the lithium fluoride target used for scoring the microdosimetric quantities and in the physical models used for the calculations, was investigated for both LiF:Mg, Ti (MTS) and LiF:Mg,Cu,P (MCP) detectors. The simulations were

repeated in case of ^1H , ^{12}C , ^{56}Fe and ^{132}Xe ions for all energies included in the study (3, 5, 7, 10, 15, 20, 30, 40, 50, 60, 70, 80, 90, 100, 125, 150, 250, 500 and 1000 MeV/u) each time changing only one simulation parameter. The first three radiation qualities were chosen for their relevance for space and hadron therapy applications, while ^{132}Xe ions were included as an extreme case being the heaviest particle included in this work. For these ions, the obtained efficiency values were then compared with ones obtained with the reference simulation parameters. The average and maximum values of the relative deviation, defined as Equation (8), were calculated for both detector types and the results are listed in Table 1.

The reference simulations were performed in a ^7Li fluoride cylinder (density = 2.5 g/cm³, diameter = 4.5 mm, thickness = 0.9 mm) neglecting the presence of dopants. The simulation cutoff for all ions was set to 1 MeV/u, the energy loss of charged particles was considered by means of the stopping power model ATIMA

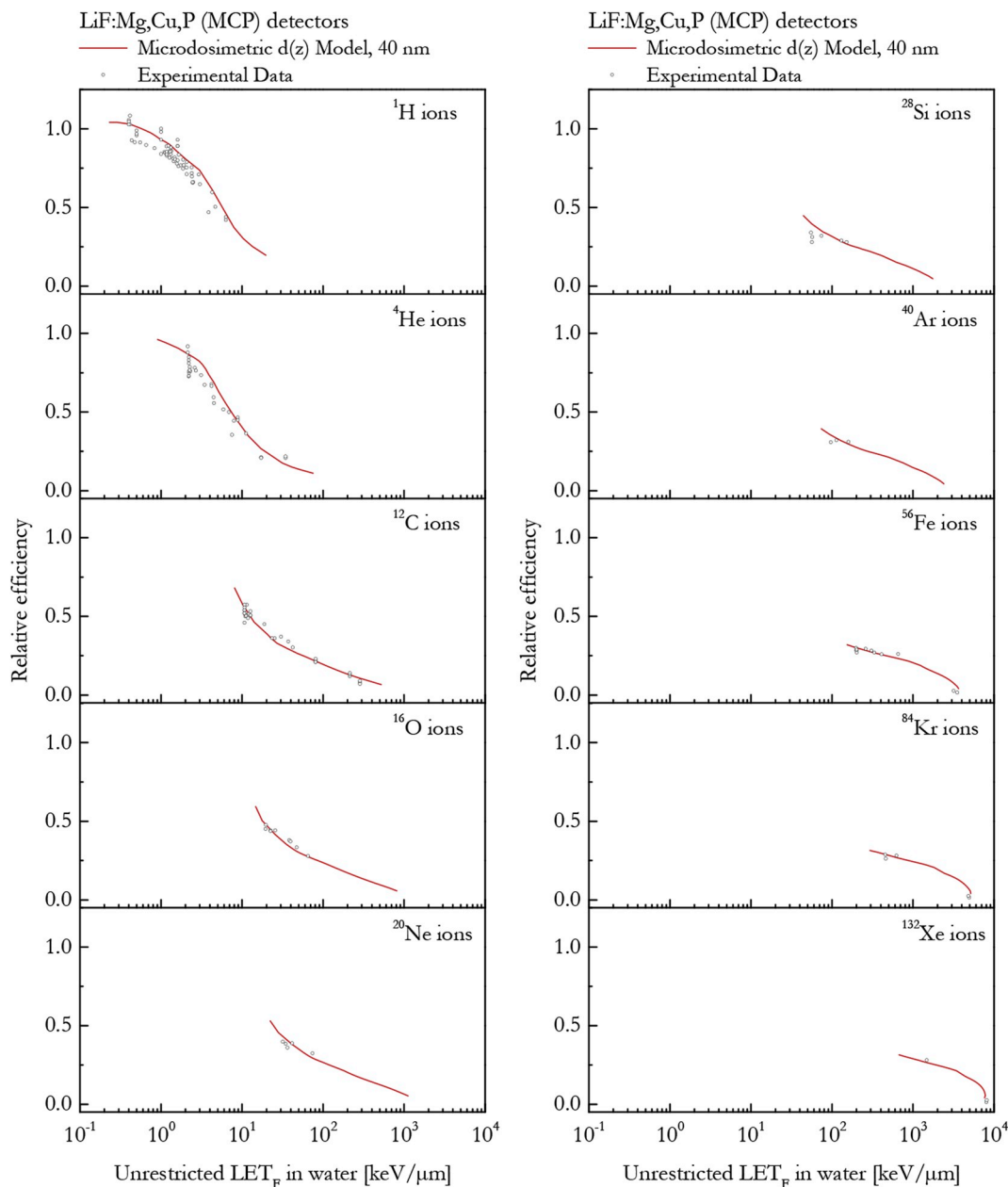


Fig. 10. Results of the Microdosimetric $d(z)$ Model in case of LiF:Mg,Cu,P (MCP) detectors for a site size of 40 nm in comparison with experimental data from Berger et al. (2006b), Bilski (2006), Berger and Hajek (2008), Bilski and Puchalska (2010), Bilski et al. (2011), Gieszczyk et al. (2013), Sądel et al. (2015b), Parisi et al. (2017) a and Parisi et al. (2018).

(<http://web-docs.gsi.de/~weick/atima>), angular and energy straggling were respectively considered using the Landau Vavilov (1957) and Lynch's Coulomb diffusion (Lynch and Dahl, 1991) formulae.

$$\text{Relative deviation} = \frac{|\eta_{\text{reference simulation}} - \eta_{\text{simulation}}|}{\eta_{\text{reference simulation}}} \quad (8)$$

3.2.1. Density of the detector

Depending on the manufacturer and the production technique, the density of these two detector types ranges from 2.5 to 2.635 g/cm³ (Horowitz, 1993; McKeever et al., 1995; Bilski, 2002). Although microdosimetry is historically based on a density scaling approach (Rossi and Zaider, 1996), the simulations were repeated to check the effect of detector density on the calculated efficiency value. As it can be seen from Table 1, this effect is negligible (around 0.4%) for both detector types.

3.2.2. Isotopic composition of lithium fluoride

Thermoluminescent detectors based on LiF:Mg, Ti (MTS) and LiF:Mg,Cu,P (MCP) can be produced with both natural or enriched lithium isotopic compositions (McKeever et al., 1995). This is done in order to enhance or suppress the sensitivity of the detectors to thermal neutrons through the nuclear reaction of Equation (9).



The calculations were repeated changing the isotopic composition of the lithium fluoride target from 100% ⁷lithium to 100% ⁶lithium. For both isotopic enrichments, the density of the detector was kept at 2.5 g/cm³. To consider the production and reaction of secondary neutrons during the charged particle simulations, the PHITS event generator (Niita et al., 2011; Sato et al., 2015) for low energy neutron interaction was activated. The average deviation between ⁶lithium and ⁷lithium based detectors was 0.28% and 0.30% for LiF:Mg, Ti (MTS) and

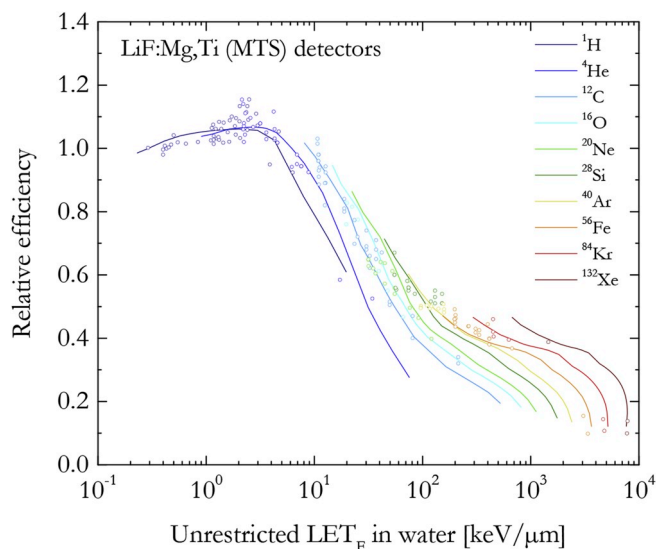


Fig. 11. Overview of the results of Microdosimetric $d(z)$ Model in case of LiF:Mg, Ti (MTS) detectors for a site size of 40 nm in comparison with experimental data from Berger et al. (2006b), Bilski (2006), Berger and Hajek (2008), Bilski and Puchalska (2010), Bilski et al. (2011), Gieszczyk et al. (2013), Sądół et al. (2015b), Parisi et al. (2017) a and Parisi et al. (2018).

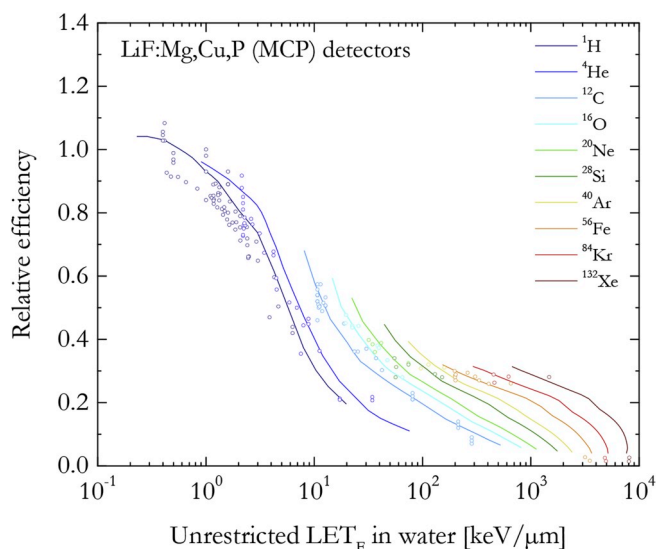


Fig. 12. Overview of the results of Microdosimetric $d(z)$ Model in case of LiF:Mg,Cu,P (MCP) detectors for a site size of 40 nm in comparison with experimental data from Berger et al. (2006b), Bilski (2006), Berger and Hajek (2008), Bilski and Puchalska (2010), Bilski et al. (2011), Gieszczyk et al. (2013), Sądół et al. (2015b), Parisi et al. (2017) a and Parisi et al. (2018).

LiF:Mg,Cu,P (MCP) respectively. Consequently, as previously experimentally observed (Bilski, 2006; Bilski et al., 2011), the charged particle efficiency of similar detectors based on different isotopic composition should be the same.

3.2.3. Diameter of the detector

Depending on the application, thermoluminescent detectors can be prepared in different dimensions and shapes (McKeever, 1988; McKeever et al., 1995). As an example, large $20 \times 20 \text{ cm}^2$ foils of LiF:Mg,Cu,P (MCP) based material were produced for two-dimensional proton therapy beam quality assurance (Gajewski et al., 2016). In order

to investigate and quantify the presence of border effects (it has to be remembered that the ratio between the perimeter and the area of the detector scales as $1/\text{radius}$), the simulations were repeated changing the diameter of the detector from 0.45 mm to 5 cm. No differences (average deviation below 0.04%) were found for both detector dimensions.

3.2.4. Dopants

It is widely accepted that dopants play a fundamental role during the trapping and recombination steps of the thermoluminescent process, affecting strongly material proprieties as glow curve structure, dose response and the efficiency in measuring different radiation qualities (McKeever et al., 1995; Lee et al., 2008; Bos, 2017). During the years, the effect of changing dopant concentrations was investigated carefully (Bilski et al., 1997, 1998; Olko et al., 2001) and, based on these results, optimized materials were produced (Nakajima et al., 1978; Horowitz, 1993; Bilski, 2002; Bilski et al., 2004 b). The reference calculations of this work were performed in an undoped lithium fluoride target. Aiming to study if the dopants could play a role also in the charged particle energy deposition process, the simulations were repeated including the nominal dopant atomic concentrations of LiF:Mg, Ti (MTS: Mg = 0.0013%, Ti = 0.012%) and LiF:Mg,Cu,P (MCP: Mg = 0.2%, P = 1.25%, Cu = 0.05%) produced at the Institute of Nuclear Physics of the Polish Academy of Science IFJ-PAN (Bilski, 2002). The dopants were assumed to be uniformly distributed within the lithium fluoride target. The results, average deviation below 0.08%, show no significant correlation between these dopant concentrations and the energy deposition process by charged particles.

3.2.5. Ion transport cutoff

In the Monte Carlo code PHITS, when a particle has energy below the cutoff value, its transport is stopped and the particle is locally absorbed (PHITS manual, <https://phits.jaea.go.jp/rireki-manuale.html>). The default cutoff value for ions is 1 MeV/u and it was used for all the reference calculations. To investigate the influence of low energy transport on the calculated efficiency values, all ion transport cutoffs were set to 1 keV/u and the simulations were repeated. The average relative deviation was found to be 0.35% and 0.41% for LiF:Mg, Ti (MTS) and LiF:Mg,Cu,P (MCP) detectors respectively. The effect is not very important because low energy particles deposit their energy in a very localized way, i.e. high specific energy distributions in the sensitive site. These high specific energy distributions are associated with very low values of the response function and contribute in a very limited way to the entire efficiency determination process.

3.2.6. Stopping power model

The energy loss of charged particles, with the only exception of electrons and positrons, was assessed by mean of the stopping power calculation model SPAR (Armstrong and Chandler, 1973) under the continuous slowing down approximation (CSDA). The latter represents the default option in PHITS until version 2.82, which is the version used for the calculations included in this work. Thanks to an improvement in the computational speed, from version 2.88 the default stopping power calculation was changed to ATIMA (<http://web-docs.gsi.de/~weick/atima>). Consequently, the calculations were performed again employing the ATIMA stopping power model. The average relative deviation was found to be 0.14% and 0.25% for LiF:Mg, Ti (MTS) and LiF:Mg,Cu,P (MCP) detectors respectively.

3.2.7. Angular and energy straggling

The effect of activating or deactivating energy, angular or both straggling options in PHITS was found to be negligible (below 0.05%) for all calculations included in this work.

Table 1

Effect of changing the simulation parameters on the calculated relative efficiency of LiF:Mg, Ti (MTS) and LiF:Mg,Cu,P (MCP).

Parameters changed from reference simulations	Average relative deviation from reference		Maximum relative deviation from reference	
	LiF:Mg,Ti (MTS)	LiF:Mg,Cu,P (MCP)	LiF:Mg,Ti (MTS)	LiF:Mg,Cu,P (MCP)
	Reference simulations = ⁷ lithium fluoride, density 2.5 g/cm ³ , diameter target 0.45 cm, SPAR stopping power model, energy and angular straggling activated, cutoffs ions = 1 MeV/u			
<i>Target definition</i>				
density = 2.635 g/cm ³	0.35%	0.40%	2.09%	2.99%
⁶ lithium fluoride	0.28%	0.30%	1.75%	3.64%
diameter = 5 cm	0.01%	0.04%	0.12%	0.79%
dopants LiF:Mg,Cu,P (MCP)	N/A	0.08%	N/A	0.91%
dopants LiF:Mg, Ti (MTS)	0.01%	N/A	0.20%	N/A
<i>Physical models</i>				
cutoffs ions = 1 keV	0.35%	0.41%	2.13%	3.08%
ATIMA stopping power model	0.14%	0.25%	3.37%	6.02%
energy straggling deactivated	0.02%	0.05%	0.24%	1.01%
angular straggling deactivated	0.01%	0.04%	0.19%	0.85%
both straggling deactivated	0.01%	0.04%	0.20%	0.94%

4. Conclusions

Due to technical limitations, the relative efficiency determination of luminescent detectors for very high and low energy particles, uncommon isotopes and exotic radiation qualities is often strongly limited. Furthermore, the assessment of detector efficiency in complex mixed fields is still very challenging. However, the use of these detectors for space and hadron therapy applications requires an accurate knowledge of their response for measuring a broad spectrum of particles and energies.

In this work, a microdosimetric model to assess the thermoluminescence efficiency was developed and successfully benchmarked in case of LiF:Mg, Ti (MTS) and LiF:Mg,Cu,P (MCP) detectors for charged particles ranging from ¹H to ¹³²Xe with energies between 3 and 1000 MeV/u. The model requires the knowledge of two ingredients: the photon dose response of the detectors and a characteristic microdosimetric site size where the microscopic energy deposition simulations should be performed. It was found that, if a site size of 40 nm is used for the calculations, the model is able to predict the efficiency of both LiF:Mg, Ti (MTS) and LiF:Mg,Cu,P (MCP) detectors in very good agreement with experimentally determined data. The determined site size is in agreement with the charge migration distance during the recombination stage (assessed to be between 40 and 47.5 nm) and the characteristic lithium fluoride crystallite size determined through X-ray diffraction (31 nm).

A sensitivity analysis was performed on the model to assess the effect of simulation parameters on the calculated efficiency values. It was found that the dimensions of the detectors, the density (ranging from 2.5 to 2.635 g/cm³ in the real detectors), the lithium isotopic composition (6- or 7- lithium) and the presence of dopants are playing a negligible role in the process. Furthermore, time consuming ion transport at energy below 1 MeV/u seems to play a very marginal role. In addition, the choice of the stopping power model (SPAR or ATIMA), the angular or the energy straggling do not affect the results.

Thus, the model will also be applied for the relative efficiency determination for a large number of combinations of particles (photons, electrons, thermal neutrons, exotic particles, antimatter ...), energies and detectors, also for mixed fields such as space or hadron therapy.

Author contribution statement

AP conceived, developed and validated the Microdosimetric d(z) Model. The other authors revised the manuscript, written by AP.

References

- Apáthy, I., Deme, S., Fehér, I., Akatov, Y.A., Reitz, G., Arkhangelski, V.V., 2002. Dose measurements in space by the Hungarian Pille TLD system. *Radiat. Meas.* 35 (5), 381–391.
- Armstrong, T.W., Chandler, K.C., 1973. SPAR, a FORTRAN program for computing stopping powers and ranges for muons, charged pions, protons, and heavy ions (No. ORNL-4869). ORNL Tenn.(USA).
- Ávila, O., Brandan, M.E., Salvat, F., Fernandez-Varea, J.M., 1996. Radial energy distributions in LiF by alpha particle irradiation using Monte Carlo simulation. *Radiat. Protect. Dosim.* 65 (1–4), 37–40.
- Ávila, O., Gamboa-deBuen, I., Brandan, M.E., 1999. Study of the energy deposition in LiF by heavy charged particle irradiation and its relation to the thermoluminescent efficiency of the material. *J. Phys. Appl. Phys.* 32 (10), 1175.
- Ávila, O., Brandan, M. E., 2002. Influence of Fd (D) on modified track structure theory efficiency calculations. *Radiat. Protect. Dosim.* 100 (1–4), 163–166.
- Ávila, O., Massillon-JL, G., Gamboa-deBuen, I., Brandan, M.E., 2008. Influence of input functions in TLD-100 ion–gamma relative efficiencies calculated with MTST. *Radiat. Meas.* 43 (2–6), 171–174.
- Bagshaw, M., 2008. Cosmic radiation in commercial aviation. *Trav. Med. Infect. Dis.* 6 (3), 125–127.
- Benton, E.R., Frank, A.L., Benton, E.V., 2000. TLD efficiency of 7LiF for doses deposited by high-LET particles. *Radiat. Meas.* 32 (3), 211–214.
- Berger, T., Hajek, M., Fugger, M., Vana, N., 2006a. Efficiency-corrected dose verification with thermoluminescence dosimeters in heavy-ion beams. *Radiat. Protect. Dosim.* 120 (1–4), 361–364.
- Berger, T., Hajek, M., Summerer, L., Fugger, M., Vana, N., 2006b. The efficiency of various thermoluminescence dosimeter types to heavy ions. *Radiat. Protect. Dosim.* 120 (1–4), 365–368.
- Berger, T., Hajek, M., 2008. TL-efficiency—overview and experimental results over the years. *Radiat. Meas.* 43 (2–6), 146–156.
- Berger, T., Meier, M., Reitz, G., Schridde, M., 2008. Long-term dose measurements applying a human anthropomorphic phantom onboard an aircraft. *Radiat. Meas.* 43 (2–6), 580–584.
- Berger, T., Hajek, M., Bilski, P., Körner, C., Vanhavere, F., Reitz, G., 2012. Cosmic radiation exposure of biological test systems during the EXPOSE-E mission. *Astrobiology* 12 (5), 387–392.
- Berger, T., Bilski, P., Hajek, M., Puchalska, M., Reitz, G., 2013. The MATROSHKA experiment: results and comparison from extravehicular activity (MTR-1) and intravehicular activity (MTR-2A/2B) exposure. *Radiat. Res.* 180 (6), 622–637.
- Berger, T., Hajek, M., Bilski, P., Reitz, G., 2015. Cosmic radiation exposure of biological test systems during the EXPOSE-R mission. *Int. J. Astrobiol.* 14 (1), 27–32.
- Berger, T., Przybyla, B., Matthia, D., Reitz, G., Burmeister, S., Labrenz, J., Bilski, P., Horwacik, T., Twardak, A., Hajek, M., Fugger, M., Hofstätter, C., Sihver, L., Palfalvi, J.K., Szabo, J., Stradi, A., Ambrozova, I., Kubancak, J., Pachnerova Brabcova, K., Vanhavere, F., Cauwels, V., Van Hoey, O., Schoonjans, W., Parisi, A., Gaza, R., Semones, E., Yukihara, E.G., Benton, E.R., Doull, B.A., Uchihori, Y., Kodaira, S., Kitamura, H., Boehme, M., 2016. DOSIS & DOSIS 3D: long-term dose monitoring onboard the Columbus laboratory of the international space station (ISS). *J. Space Weather Space Climate* 6, A39.
- Bilski, P., Budzanowski, M., Olko, P., 1997. Dependence of LiF: Mg, Cu, P (MCP-N) glow-curve structure on dopant composition and thermal treatment. *Radiat. Protect. Dosim.* 69 (3), 187–198.
- Bilski, P., Budzanowski, M., Olko, P., Waligorski, M.P.R., 1998. Influence of concentration of magnesium on the dose response and LET-dependence of TL efficiency in LiF: Mg, Cu, P (MCP-N) detectors. *Radiat. Meas.* 29 (3–4), 355–359.

- Bilski, P., Budzanowski, M., 2001. Self-attenuation of TL light from LiF—a comparison of different experimental methods. *Radiat. Meas.* 33 (5), 679–685.
- Bilski, P., 2002. Lithium fluoride: from LiF: Mg, Ti to LiF: Mg, Cu, P. *Radiat. Protect. Dosim.* 100 (1–4), 199–205.
- Bilski, P., Olko, P., Horwacik, T., 2004 a. Air-crew exposure to cosmic radiation on board of Polish passenger aircraft. *Nukleonika* 49 (2), 77–83.
- Bilski, P., Budzanowski, M., Olko, P., Mandowska, E., 2004 b. LiF: Mg, Ti (MTT) TL detectors optimised for high-LET radiation dosimetry. *Radiat. Meas.* 38 (4–6), 427–430.
- Bilski, P., 2006. Response of various LiF thermoluminescent detectors to high energy ions—Results of the ICCHIBAN experiment. *Nucl. Instrum. Methods Phys. Res. Sect. B Beam Interact. Mater. Atoms* 251 (1), 121–126.
- Bilski, P., Olko, P., Puchalska, M., Obryk, B., Waligórski, M.P.R., Kim, J.L., 2007. High-dose characterization of different LiF phosphors. *Radiat. Meas.* 42 (4–5), 582–585.
- Bilski, P., Puchalska, M., 2010. Relative efficiency of TL detectors to energetic ion beams. *Radiat. Meas.* 45 (10), 1495–1498.
- Bilski, P., Berger, T., Hajek, M., Reitz, G., 2011. Comparison of the response of various TLDs to cosmic radiation and ion beams: current results of the HAMLET project. *Radiat. Meas.* 46 (12), 1680–1685.
- Bos, A.J., 2017. Thermoluminescence as a Research tool to investigate luminescence mechanisms. *Materials* 10 (12), 1357.
- Boscolo, D., Scifoni, E., Carlino, A., La Tessa, C., Berger, T., Durante, M., Rosso, V., Krämer, M., 2015. TLD efficiency calculations for heavy ions: an analytical approach. *Europ. Phys. J. D* 69 (12), 286.
- Butts, J., Katz, R., 1967. Theory of RBE for heavy ion bombardment of dry enzymes and viruses. *Radiat. Res.* 30 (4), 855–871.
- Chatterjee, A., Schaefer, H.J., 1976. Microdosimetric structure of heavy ion tracks in tissue. *Radiat. Environ. Biophys.* 13 (3), 215–227.
- Chen, J., Kellner, A.M., 1997. Calculation of radial dose distributions for heavy ions by a new analytical approach. *Radiat. Protect. Dosim.* 70 (1–4), 55–58.
- Chen, R., Pagonis, V., 2011. Thermally and Optically Stimulated Luminescence: a Simulation Approach.
- Cucinotta, F.A., Wilson, J.W., Shavers, M.R., Katz, R., 1997. Calculation of Heavy Ion Inactivation and Mutation Rates in Radial Dose Model of Track Structure.
- Deme, S., Apathy, I., Hejja, I., Lang, E., Feher, I., 1999. Extra dose due to extravehicular activity during the NASA4 mission, measured by an on-board TLD system. *Radiat. Protect. Dosim.* 85 (1–4), 121–124.
- Faïn, J., Monnin, M., Montret, M., 1974. Spatial energy distribution around heavy-ion path. *Radiat. Res.* 57 (3), 379–389.
- Gajewski, J., Kłosowski, M., Olko, P., 2016. Two-dimensional thermoluminescence dosimetry system for proton beam quality assurance. *Radiat. Meas.* 90, 224–227.
- Gamboa-deBuen, I., Buenfil, A.E., Ruiz, C.G., Rodriguez-Villafuerte, M., Flores, A., Brandan, M.E., 1998. Thermoluminescent response and relative efficiency of TLD-100 exposed to low-energy x-rays. *Phys. Med. Biol.* 43 (8), 2073.
- Geiß, O.B., Krämer, M., Kraft, G., 1998 a. Efficiency of thermoluminescent detectors to heavy charged particles. *Nucl. Instrum. Methods Phys. Res. Sect. B Beam Interact. Mater. Atoms* 142 (4), 592–598.
- Geiß, O.B., Krämer, M., Kraft, G., 1998 b. Verification of heavy ion dose distributions using thermoluminescent detectors. *Nucl. Instrum. Methods Phys. Res. Sect. B Beam Interact. Mater. Atoms* 146 (1–4), 541–544.
- Gieszczyk, W., Bilski, P., Olko, P., Herrmann, R., Kettunen, H., Virtanen, A., Bassler, N., 2013. Evaluation of the relative thermoluminescence efficiency of LiF: Mg, Ti and LiF: Mg, Cu, P TL detectors to low-energy heavy ions. *Radiat. Meas.* 51, 7–12.
- Greilich, S., Hahn, U., Kiderlen, M., Andersen, C.E., Bassler, N., 2014. Efficient calculation of local dose distributions for response modeling in proton and heavier ion beams. *Europ. Phys. J. D* 68 (10), 327.
- Hajek, M., Berge, T., Schöner, W., Summerer, L., Vana, N., 2002. Dose assessment of aircrew using passive detectors. *Radiat. Protect. Dosim.* 100 (1–4), 511–514.
- Hajek, M., Berger, T., Vana, N., 2004. A TLD-based personal dosimeter system for aircrew monitoring. *Radiat. Protect. Dosim.* 110 (1–4), 337–341.
- Hajek, M., Berger, T., Fugger, M., Fürstner, M., Vana, N., Akatov, Y., Shurshakov, V., Arkhangelsky, V., 2006. Dose distribution in the Russian segment of the international space station. *Radiat. Protect. Dosim.* 120 (1–4), 446–449.
- Hirayama, H., Namito, Y., Nelson, W.R., Bielajew, A.F., Wilderman, S.J., 2005. The EGS5 Code System (No. SLAC-R-730).
- Horowitz, Y.S., 1981. The theoretical and microdosimetric basis of thermoluminescence and applications to dosimetry. *Phys. Med. Biol.* 26 (5), 765.
- Horowitz, Y.S., 1990. Mathematical modelling of TL supralinearity for heavy charged particles. *Radiat. Protect. Dosim.* 33 (1–4), 75–81.
- Horowitz, Y.S., 1993. LiF: Mg, Ti versus LiF: Mg, Cu, P: the competition heats up. *Radiat. Protect. Dosim.* 47 (1–4), 135–141.
- Horowitz, Y.S., Rosenkrantz, M., Mahajna, S., Yossian, D., 1996. The track interaction model for alpha particle induced thermoluminescence supralinearity: dependence of the supralinearity on the vector properties of the alpha particle radiation field. *J. Phys. Appl. Phys.* 29 (1), 205.
- Horowitz, Y.S., Siboni, D., Oster, L., Livingstone, J., Guatelli, S., Rosenfeld, A., Emfietzoglou, D., Bilski, P., Obryk, B., 2012. Alpha particle and proton relative thermoluminescence efficiencies in LiF: Mg, Cu, P: is track structure theory up to the task? *Radiat. Protect. Dosim.* 150 (3), 359–374.
- Horowitz, Y.S., 1999. The average distance between Mg-based trapping structures in LiF: Mg, Ti and LiF: Mg, Cu, P and the relevance to microdosimetry. *Radiat. Protect. Dosim.* 82 (1), 51–54.
- Horowitz, Y.S., 2001. Theory of thermoluminescence gamma dose response: the unified interaction model. *Nucl. Instrum. Methods Phys. Res. Sect. B Beam Interact. Mater. Atoms* 184 (1–2), 68–84.
- Hubbell, J.L., Seltzer, S.M., 2004. Tables of X-Ray Mass Attenuation Coefficients and Mass Energy-absorption Coefficients from 1 KeV to 20 MeV for Elements Z = 1 to 92 and 48 Additional Substances of Dosimetric Interest (version 1.4). National Institute of Standards and Technology, Gaithersburg, MD Available online at: <http://physics.nist.gov/xaamdi>.
- Hutchison, C.A., Johnston, H.L., 1940. Determination of crystal densities by the temperature of flotation method. Density and lattice constant of lithium fluoride. *J. Am. Chem. Soc.* 62 (11), 3165–3168.
- International Commission on Radiation Units and Measurements, 1970. ICRU Report 16 Linear Energy Transfer.
- International Commission on Radiation Units and Measurements, 1983. ICRU Report 36 Microdosimetry.
- Kalef-Ezra, J., Horowitz, Y.S., 1982. Heavy charged particle thermoluminescence dosimetry: track structure theory and experiments. *Int. J. Appl. Radiat. Isot.* 33 (11), 1085–1100.
- Katona, T., Osvay, M., Deme, S., Kovacs, A., 2007. Environmental dosimetry using high-sensitivity TL detectors. *Radiat. Phys. Chem.* 76 (8–9), 1511–1514.
- Katz, R., Loh, K.S., Daling, L., Huang, G.R., 1990. An analytic representation of the radial distribution of dose from energetic heavy ions in water, Si, LiF, NaI, and SiO₂. *Radiat. Eff. Defect Solid* 114 (1–2), 15–20.
- Katz, R., Cucinotta, F.A., Zhang, C.X., 1996. The calculation of radial dose from heavy ions: predictions of biological action cross sections. *Nucl. Instrum. Methods Phys. Res. Sect. B Beam Interact. Mater. Atoms* 107 (1–4), 287–291.
- Kellner, A.M., 1985. Fundamentals of microdosimetry. The dosimetry of ionizing radiation 1, 77–162.
- Knežević, Ž., Ambrozova, I., Domingo, C., Saint-Hubert, D., Majer, M., Martínez-Rovira, I., Miljanić, S., Mojżeszek, N., Porwół, P., Ploc, O., Romero-Expósito, M., Stolarczyk, L., Trinkl, S., Harrison, R.M., Olko, P., 2017. Comparison of response of passive dosimetry systems in scanning proton radiotherapy—a study using paediatric anthropomorphic phantoms. *Radiat. Protect. Dosim.* 1–5.
- Krämer, M., Kraft, G., 1994. Calculations of heavy-ion track structure. *Radiat. Environ. Biophys.* 33 (2), 91–109.
- Kron, T., 1999. Applications of thermoluminescence dosimetry in medicine. *Radiat. Protect. Dosim.* 85 (1–4), 333–340.
- Kunst, J., Kopeć, R., Kukołowicz, P., Mojżeszek, N., Sadowski, B., Stolarczyk, L., Ślusarczyk-Kacprzyk, W., Tobiła, A., Olko, P., 2017. Mailed dosimetric audit of therapeutic proton beams using thermoluminescence MTS-N (LiF: Mg, Ti) powder—First results. *Radiat. Meas.* 106, 312–314.
- Lappa, A.V., Bigildeev, E.A., Burmistrov, D.S., Vasilyev, O.N., 1993. “Trion” code for radiation action calculations and its application in microdosimetry and radiobiology. *Radiat. Environ. Biophys.* 32 (1), 1–19.
- Larsson, L., Katz, R., 1976. Supralinearity of thermoluminescent dosimeters. *Nucl. Instrum. Methods* 138 (4), 631–636.
- Lee, J.I., Kim, J.L., Pradhan, A.S., Kim, B.H., Chung, K.S., Choe, H.S., 2008. Role of dopants in LiF TLD materials. *Radiat. Meas.* 43 (2–6), 303–308.
- Lynch, G.R., Dahl, O.L., 1991. Approximations to multiple Coulomb scattering. *Nucl. Instrum. Methods Phys. Res. Sect. B Beam Interact. Mater. Atoms* 58 (1), 6–10.
- Massillon-Jl, G., Gamboa-deBuen, I., Brandan, M.E., 2006. Onset of supralinear response in TLD-100 exposed to 60Co gamma-rays. *J. Phys. Appl. Phys.* 39 (2), 262.
- Massillon-Jl, G., Ávila, O., Brandan, M.E., 2011. Supralinear response of LiF: Mg, Ti (TLD-100) after exposure to 100 keV average energy X-rays. *Radiat. Meas.* 46 (12), 1357–1360.
- Mayles, P., Nahum, A., Rosenwald, J.C., 2007. Handbook of Radiotherapy Physics: Theory and Practice. CRC Press.
- McKeever, S.W., 1988. Thermoluminescence of Solids, vol. 3 Cambridge University Press.
- McKeever, S.W., Moscovitch, M., Townsend, P.D., 1995. Thermoluminescence Dosimetry Materials: Properties and Uses.
- Moliere, G., 1948. Theorie der streuung schneller geladener teilchen ii mehrfach-und vielfachstreuung. *Z. Naturforsch.* 3 (2), 78–97.
- Mukherjee, B., Lambert, J., Hentschel, R., Farr, J., 2011. Explicit estimation of out-of-field neutron and gamma dose equivalents during proton therapy using thermoluminescence-dosimeters. *Radiat. Meas.* 46 (12), 1952–1955.
- Nakajima, T., Murayama, Y., Matsuzawa, T., Koyano, A., 1978. Development of a new highly sensitive LiF thermoluminescence dosimeter and its applications. *Nucl. Instrum. Methods* 157 (1), 155–162.
- Nelson, G.A., 2016. Space radiation and human exposures, a primer. *Radiat. Res.* 185 (4), 349–358.
- Niita, K., Sato, T., Iwase, H., Nose, H., Nakashima, H., Sihver, L., 2006. PHITS—a particle and heavy ion transport code system. *Radiat. Meas.* 41 (9–10), 1080–1090.
- Niita, K., Iwamoto, Y., Sato, T., Matsuda, N., Sakamoto, Y., Nakashima, H., Iwase, H., Sihver, L., 2011. Event generator models in the particle and heavy ion transport code system; PHITS. *J. Kor. Phys. Soc.* 59 (2), 827–832.
- Olko, P., 1989. Fluctuations of Energy Deposited in Biological Targets by Ionizing Radiation (Doctoral Dissertation). PhD thesis. Institute of Medicine, KFA Jülich.
- Olko, P., Booz, J., 1990. Energy deposition by protons and alpha particles in spherical sites of nanometer to micrometer diameter. *Radiat. Environ. Biophys.* 29 (1), 1–17.
- Olko, P., Bilski, P., Budzanowski, M., Molokanov, A., Ochab, E., Waligórski, M.P.R., 2001. Supralinearity of peak 4 and 5 in thermoluminescent lithium fluoride MTS-N (LiF: Mg, Ti) detectors at different Mg and Ti concentration. *Radiat. Meas.* 33 (5), 807–812.
- Olko, P., 2002 a. Microdosimetric Modelling of Physical and Biological Detectors (Habilitation Thesis). Henryk Niewodniczański Institute of Nuclear Physics.
- Olko, P., 2002 b. The microdosimetric one-hit detector model for calculating the response of solid state detectors. *Radiat. Meas.* 35 (3), 255–267.
- Olko, P., Waligórski, M.P.R., 2002. Microdosimetric one hit detector model for calculation of dose and energy response of some solid state detectors. *Radiat. Protect. Dosim.* 99 (1–4), 381–382.

- Olko, P., Bilski, P., Kim, J.L., 2002 a. Microdosimetric interpretation of the photon energy response of LiF: Mg, Ti detectors. *Radiat. Protect. Dosim.* 100 (1–4), 119–122.
- Olko, P., Bilski, P., Budzanowski, M., Waligórski, M.P.R., Reitz, G., 2002 b. Modeling the response of thermoluminescence detectors exposed to low-and high-LET radiation fields. *J. Radiat. Res.* 43 (S), S59–S62.
- Olko, P., 2004. Microdosimetric modelling of the relative efficiency of thermoluminescent materials. *Radiat. Meas.* 38 (4–6), 781–786.
- Olko, P., Bilski, P., Budzanowski, M., Molokanov, A., 2004. Dosimetry of heavy charged particles with thermoluminescence detectors—models and applications. *Radiat. Protect. Dosim.* 110 (1–4), 315–318.
- Olko, P., Bilski, P., El-Faramawy, N.A., Göksoy, H.Y., Kim, J.L., Kopec, R., Waligorski, M.P.R., 2006. On the relationship between dose-, energy-and LET-response of thermoluminescent detectors. *Radiat. Protect. Dosim.* 119 (1–4), 15–22.
- Olko, P., 2007. Microdosimetry, track structure and the response of thermoluminescence detectors. *Radiat. Meas.* 41, S57–S70.
- Olko, P., 2010. Advantages and disadvantages of luminescence dosimetry. *Radiat. Meas.* 45 (3–6), 506–511.
- Paretzke, H.G., 1988. In: Freeman, G.R. (Ed.), *Radiation Track Structure Theory in Kinetics of Nonhomogeneous Processes*. John Wiley & Sons, New York.
- Parisi, A., Van Hoey, O., Mégret, P., Vanhavere, F., 2017 a. The influence of the dose assessment method on the LET dependence of the relative luminescence efficiency of LiF: Mg, Ti and LiF: Mg, Cu, P. *Radiat. Meas.* 98, 34–40.
- Parisi, A., Van Hoey, O., Mégret, P., Vanhavere, F., 2017 b. Deconvolution study on the glow curve structure of LiF: Mg, Ti and LiF: Mg, Cu, P thermoluminescent detectors exposed to 1H, 4He and 12C ion beams. *Nucl. Instrum. Methods Phys. Res. Sect. B Beam Interact. Mater. Atoms* 407, 222–229.
- Parisi, A., Van Hoey, O., Vanhavere, F., 2017 c. Microdosimetric modeling of the relative luminescence efficiency of LiF:Mg,Ti (MTS) detectors exposed to charged particles. *Radiat. Protect. Dosim.* 1–4.
- Parisi, A., Van Hoey, O., Mégret, P., Vanhavere, F., 2017 d. Microdosimetric modeling of the relative luminescence efficiency of LiF:Mg,Cu,P (MCP) detectors exposed to charged particles. *Radiat. Protect. Dosim.* accepted for publication.
- Parisi, A., de Freitas Nascimento, L., Van Hoey, O., Mégret, P., Kitamura, H., Kodaira, S., Vanhavere, F., 2018. Low temperature thermoluminescence anomaly of LiF:Mg,Cu,P radiation detectors exposed to 1H and 4He ions. *Radiat. Meas.* accepted for publication.
- Reitz, G., Beaujean, R., Benton, E., Burmeister, S., Dachev, T., Deme, S., Luszik-Bhadra, M., Olko, P., 2005. Space radiation measurements on-board ISS—the DOSMAP experiment. *Radiat. Protect. Dosim.* 116 (1–4), 374–379.
- Roomi, S., Ali, S., Ahmad, H., Hayat, K., Zulfiqar, S., Iqbal, Y., 2018. Development of a new rare-earth (Dy 3+) based thermoluminescent dosimeter. *J. Lumin.* 196, 373–378.
- Rossi, H.H., Biavati, M.H., Gross, W., 1961. Local energy density in irradiated tissues: I. Radiobiological significance. *Radiat. Res.* 15 (4), 431–439.
- Rossi, H.H., Zaider, M., 1996. *Microdosimetry and its Applications*. Springer-Verlag Berlin Heidelberg.
- Sato, T., Watanabe, R., Niita, K., 2006. Development of a calculation method for estimating specific energy distribution in complex radiation fields. *Radiat. Protect. Dosim.* 122 (1–4), 41–45.
- Sato, T., Watanabe, R., Kase, Y., Tsuruoka, C., Suzuki, M., Furusawa, Y., Niita, K., 2010. Analysis of cell-survival fractions for heavy-ion irradiations based on microdosimetric kinetic model implemented in the particle and heavy ion transport code system. *Radiat. Protect. Dosim.* 143 (2–4), 491–496.
- Sato, T., Furusawa, Y., 2012. Cell survival fraction estimation based on the probability densities of domain and cell nucleus specific energies using improved microdosimetric kinetic models. *Radiat. Res.* 178 (4), 341–356.
- Sato, T., Watanabe, R., Sihver, L., Niita, K., 2012. Applications of the microdosimetric function implemented in the macroscopic particle transport simulation code PHITS. *Int. J. Radiat. Biol.* 88 (1–2), 143–150.
- Sato, T., Niita, K., Matsuda, N., Hashimoto, S., Iwamoto, Y., Noda, S., Ogawa, T., Iwase, H., Nakashima, H., Fukahori, T., Okumura, K., 2013. Particle and heavy ion transport code system, PHITS, version 2.52. *J. Nucl. Sci. Technol.* 50 (9), 913–923.
- Sato, T., Hamada, N., 2014. Model assembly for estimating cell surviving fraction for both targeted and nontargeted effects based on microdosimetric probability densities. *PLoS One* 9 (11), e114056.
- Sato, T., Niita, K., Matsuda, N., Hashimoto, S., Iwamoto, Y., Furuta, T., Noda, S., Ogawa, T., Iwase, H., Nakashima, H., Fukahori, T., 2015. Overview of particle and heavy ion transport code system PHITS. *Ann. Nucl. Energy* 82, 110–115.
- Sato, T., Iwamoto, Y., Hashimoto, S., Ogawa, T., Furuta, T., Abe, S.I., Kai, T., Tsai, P.E., Matsuda, N., Iwase, H., Shigyo, N., 2018. Features of particle and heavy ion transport code system (PHITS) version 3.02. *J. Nucl. Sci. Technol.* 1–7.
- Şaşel, M., Bilski, P., Swakoń, J., Weber, A., 2015a. Evaluation of the relative TL efficiency of the thermoluminescent detectors to heavy charged particles. *Radiat. Protect. Dosim.* 168 (1), 27–32.
- Şaşel, M., Bilski, P., Swakoń, J., Rydygier, M., Horwacik, T., Weber, A., 2015b. Comparative investigations of the relative thermoluminescent efficiency of LiF detectors to protons at different proton therapy facilities. *Radiat. Meas.* 82, 8–13.
- Stolarczyk, L., Trinkl, S., Romero-Exposito, M., Mojżeszczak, N., Ambrozova, L., Domingo, C., Davidková, M., Farah, J., Kłodowska, M., Knežević, Ž., Liszka, M., 2018. Dose distribution of secondary radiation in a water phantom for a proton pencil beam-EURADOS WG9 intercomparison exercise. *Phys. Med. Biol.* 63 (8), 085017.
- Straube, U., Berger, T., Reitz, G., Facius, R., Fuglesang, C., Reiter, T., Damann, V., Tognini, M., 2010. Operational radiation protection for astronauts and cosmonauts and correlated activities of ESA Medical Operations. *Acta Astronaut.* 66 (7–8), 963–973.
- Szántó, P., Apáthy, I., Deme, S., Hirn, A., Nikolaev, I.V., Pázmándi, T., Shurshakov, V.A., Tolochek, R.V., Yarmanova, E.N., 2015. Onboard cross-calibration of the Pille-ISS Detector System and measurement of radiation shielding effect of the water filled protective curtain in the ISS crew cabin. *Radiat. Meas.* 82, 59–63.
- Tomita, H., Kai, M., Kusama, T., Ito, A., 1997. Monte Carlo simulation of physicochemical processes of liquid water radiolysis. *Radiat. Environ. Biophys.* 36 (2), 105–116.
- Tsuda, S., Sato, T., Takahashi, F., Satoh, D., Sasaki, S., Namito, Y., Iwase, H., Ban, S., Takada, M., 2012. Systematic measurement of lineal energy distributions for proton, He and Si ion beams over a wide energy range using a wall-less tissue equivalent proportional counter. *J. Radiat. Res.* 53 (2), 264–271.
- Tsuda, S., Sato, T., Ogawa, T., Sasaki, S., 2016. Review of the microdosimetric studies for high-energy charged particle beams using a tissue-equivalent proportional counter. In: *Proceedings of International Symposium on Radiation Detectors and Their Uses (ISR2016)*, id. 060004, 6 pp. (No. 6).
- Turner, J.E., Hamm, R.N., Wright, H.A., Modolo, J.T., Sordi, G.M.A.A., 1980. Monte Carlo calculation of initial energies of Compton electrons and photoelectrons in water irradiated by photons with energies up to 2 MeV. *Health Phys.* 39 (1), 49–55.
- Vanhavere, F., Genicot, J.L., O’Sullivan, D., Zhou, D., Spurný, F., Jadrničková, I., Sawakuchi, G.O., Yukihara, E.G., 2008. Dosimetry of Biological Experiments in Space (DOBIES) with luminescence (OSL and TL) and track etch detectors. *Radiat. Meas.* 43 (2–6), 694–697.
- Vavilov, P.V., 1957. Ionization losses of high-energy heavy particles. *Zh. Eksp. Teor. Fiz.* 32, 749–751.
- Waligórski, M.P., Katz, R., 1980. Supralinearity of peak 5 and peak 6 in TLD-700. *Nucl. Instrum. Methods* 172 (3), 463–470.
- Waligórski, M.P.R., Hamm, R.N., Katz, R., 1986. The radial distribution of dose around the path of a heavy ion in liquid water. *Int. J. Radiat. Appl. Instrum. Nucl. Tracks Radiat. Meas.* 11 (6), 309–319.
- Yasuda, H., 2009. Effective dose measured with a life size human phantom in a low Earth orbit mission. *J. Radiat. Res.* 50 (2), 89–96.
- Zábori, B., Hirn, A., Deme, S., Apáthy, I., Csöke, A., Pázmándi, T., Szántó, P., 2016. Space dosimetry measurements in the stratosphere using different active and passive dosimetry systems. *Radiat. Protect. Dosim.* 171 (4), 453–462.
- Ziegler, James F., Ziegler, Matthias D., Biersack, Jochen P., 2010. SRIM—The stopping and range of ions in matter. *Nucl. Instrum. Methods Phys. Res. Sect. B Beam Interact. Mater. Atoms* 268 (11–12), 1818–1823 2010.